Submitted to *Advance in Space Research (Revision version 2)*

Lagrangian analysis of satellite-derived currents: Application to the North Western Mediterranean coastal dynamics

Jerome Bouffard[a], Francesco Nencioli[a], Romain Escudier[b], Andrea Michelangelo Doglioli[a], Anne Petrenko[a], Ananda Pascual[b], Pierre-Marie Poulain[c] and Dalila Elhmaidi[d]

[a] Aix Marseille Université, CNRS/INSU, IRD, Mediterranean Institute of Oceanography (MIO), UM 110, 13288 Marseille
Université de Toulon, CNRS/INSU, IRD, Mediterranean Institute of Oceanography (MIO), UM 110, 83957 La Garde

[b] IMEDEA (CSIC-UIB), Esporles, Spain

[c] OGS, Trieste, Italy

[d] Faculté des Sciences de Tunis-Université de Tunis El Manar, Tunisia

Abstract

Optimal interpolation methods for improving the reconstruction of coastal dynamics from along-track satellite altimetry measurements have been recently developed over the North Western Mediterranean Sea. Maps of satellite-derived geostrophic current anomalies are generated using these methods, and added to different mean circulation fields in order to obtained absolute geostrophic currents. The resulting fields are then compared to standard AVISO products, and their accuracies are assessed with Lagrangian diagnostics. The trajectories of virtual particle clusters are simulated with a Lagrangian code either with new current fields or with the AVISO ones. The simulated trajectories are then compared to 16 *in situ* drifter trajectories to evaluate the performance of the different velocity fields. The comparisons show that the new current fields lead to better results than the AVISO one, especially over the shallow continental shelf of the Gulf of Lion. However, despite the use of innovative strategies, some altimetry limitations still persist in the coastal domain, where small scale processes remain sub-sampled by conventional altimetry coverage but will benefit from technological development in the near future. Some of the limitations of the Lagrangian diagnostics presently used are also analyzed, but dedicated studies will be required for future further investigations.

Key words: Lagrangian diagnostics, satellite altimetry, mean dynamic topography, coastal dynamics

Corresponding author: BOUFFARD Jérôme

M.I.O. Institut Méditerranéen d'Océanologie , Campus de Luminy, Case 901 , 13288 MARSEILLE cedex 09, Etg: 6, Bât: TPR2

Mail : Jerome.Bouffard@univ-amu.fr

Tel : +33491829108

1. Introduction

Coastal regions are characterized by a complex dynamics, often dominated by small, rapidly evolving structures at the mesoscale. In the open ocean, mesoscale dynamics plays a key role in modulating large-scale circulation and heat fluxes as well as in enhancing primary production (McGillicuddy et al., 2007). Such hydrodynamic processes are also crucial at coastal scales, where the associated currents are known to significantly influence water-mass mixing and exchanges between the continental shelf and the open ocean (Huthnance, 1995).

The high spatial/temporal variability and complexity associated with coastal mesoscale processes make them difficult to be studied with sparse *in situ* observations. Alternative options rely on exploiting satellite data specifically adapted to the coastal domain. Satellite altimeters are well adapted to observe open-ocean mesoscale structures (Fu et al., 2010) and represent an invaluable source of data that provides repetitive views of phenomena unachievable by other means (Fu and Chelton, 2001). Characterizing the influence of mesoscale dynamics on water-mass stirring, mixing and tracer transport based on satellite observations is still a challenging issue, and requires the development of diagnostics that combine 2D current fields coupled with Lagrangian tools.

Optimal interpolation of along-track altimetry Sea Level Anomaly (SLA) into 2D fields was originally based on the combination of 2 altimeter missions, which could not fully resolve dynamical features at scales of 10-100 km (Le Traon and Dibarboure, 2004). Nowadays, despite using 4 altimetry missions, the resulting AVISO regional maps (SSALTO-DUACS, 2006) may still smooth a large part of mesoscale signals, especially in the coastal domain where the spatial horizontal scales are known to be smaller and more anisotropic than in the open ocean.

This has been confirmed by recent studies which evidenced that Map of SLA (hereafter (M)SLA) still lack enough of the temporal and spatial resolution and/or accuracy required for the detection of small mesoscale features (horizontal scales of less than 50 km; Bouffard et al., 2012). Furthermore, Nencioli et al. (2011) have identified inconsistencies between surface transport patterns derived from altimetry in the western Gulf of Lion and the *in situ* structures detected through an adaptative sampling strategy, which combined ship-based ADCP velocities and Lagrangian drifter trajectories. Finally, using glider measurements, Pascual et al. (2010) as well as Bouffard et al. (2010) also highlighted limitations of standard AVISO gridded fields in characterizing coastal mesoscale dynamics.

In order to improve altimetry gridded fields, a series of alternative methods have been recently developed. For example, Gaultier et al. (2013) have exploited the information from oceanic submesoscale structures retrieved from tracer observations of sea surface temperature, in order to improve the characterization of mesoscale dynamics from altimetric (M)SLA. Dussurget et al. (2011) successfully applied another technique consisting in removing the large scale signals (~100 km) from along track altimetric data and then mapping and adding the residual with an Optimal Interpolation (OI) with regionally adjusted correlation scales.

Another critical aspect for the reconstruction of coastal mesoscale dynamics may concern the inaccuracies of the Mean Dynamic Topography (hereafter MDT) associated with the marine geoid. Although the marine geoid component dominates the altimetry signal, it is not known well enough to be removed independently. Therefore, a temporal mean altimeter height is usually constructed from several year-long time series and subtracted to eliminate the geoid component. This procedure removes not only the geoid component but also any current component with a non-zero mean. So, a MDT, i.e. the non static component of the stationary sea surface height, is generally added to the (M)SLA in order to derive absolute geostrophic currents. The AVISO products in the Mediterranean Sea typically use the MDT from Rio et al. (2007).

The analysis of satellite-based mesoscale dynamics and its impact on horizontal mixing and transport properties in the coastal domain requires not only the use of new satellite-derived fields but also relevant diagnostics in order to evaluate them. None of the previous studies (Dussurget et al., 2011; Gaultier et al., 2013; Escudier et al., 2013) have focused on the quantification of the impact of different OI methods and MDT products on altimetry-based approaches. This paper addresses this issue by applying an improved Lagrangian diagnostics to several satellite-derived velocity fields, regionally adapted to the North Western Mediterranean basin.

The major dynamical feature of the North Western Mediterranean (hereafter NWMed) is the so-called “Northern Current” (hereafter NC). As shown on Figure 1, this density current arises from the junction of the Eastern and Western Corsica Current (respectively ECC and WCC on Figure 1) and flows westward initially along the coast of the Ligurian Sea, and then along the continental slope of the Gulf of Lion, until it reaches the Balearic Sea (Millot, 1991). The NC is marked by a strong seasonal variability (Gostan, 1967). Over the Gulf of Lion (hereafter GoL), NC intrusions can bring open Mediterranean water onto the continental shelf, depending on the stratification and wind conditions (Millot, 1990; Gatti, 2008; Petrenko et al. 2005, 2008; Poulain et al., 2012b). Another key aspect related to the NC dynamics concerns the development of baroclinic and barotropic instabilities. These favor the development of coastal mesoscale structures such as meanders and eddies arising along the NC external and internal border, forced by strong wind events and/or bottom topography irregularities (Millot, 1991).

Figure 1

The NC mean position is within 50 km off the coast (Petrenko et al., 2003), where radiometer and altimeter footprints may encounter the coastline and corrupt the raw along-track remote-sensed signals (Anzenhofer et al., 1999; Strub, 2001). However, recent advances in altimetry data processing can be used to characterize small scale signals in coastal regions, specifically over the NWMed (Vignudelli et al., 2003; 2005; Bouffard et al., 2008a,b; 2010; 2011, 2012). Birol et al. (2010) analyzed ADCP current measurements and satellite across-track current anomalies at different locations on the NWMed shelf edge. The results indicated good altimeter performances at seasonal time scales, confirming that improved coastal along-track altimetry is reliable to observe low frequency variations of the NC dynamics. Along-track data have also allowed to observe the NC intrusions over the GoL continental shelf for the first time (Bouffard et al., 2011) and to characterize the inter-annual (Bouffard, 2007; Birol et al., 2010) and intra seasonal (Bouffard et al., 2008b) variability of coastal currents.

Despite such major advances in coastal altimetry (in the NWMed as well as in many other areas; refer to Vignudelli et al., 2011 for an exhaustive review), most of the studies were based on Eulerian analysis of along-track altimetric measurements from which it is impossible to precisely identify and monitor in space and time coherent mesoscale features. The main objective of this study is therefore to evaluate the improvements in new coastal gridded currents through Lagrangian analysis. In particular, this work aims at assessing, for the first time, the impact of different OI methods combined with mean currents from different MDT products. This is achieved by comparing the real trajectories of drifters launched in the summers 2008, 2009 and 2010 with clusters of virtual particles advected by the different velocity fields.

The paper is organized as follow: Firstly, we present the different datasets (altimetry and drifters) and the metrics used to compute the Lagrangian trajectories from the altimetry products. Secondly, the trajectories are used to derive a Lagrangian diagnostics, whose statistics are analyzed over the NWMed basins, with a specific focus over the GoL continental shelf. Then, we discuss the ability of optimized altimetric gridded fields to reproduce specific mesoscale features identified by *in situ* observations and model results but not by standard AVISO velocity fields.

1. Material and methods

2.1 Altimetric geostrophic current anomalies

In this paper, two kinds of (M)SLA products derived from different OI methods are used and evaluated :

- The AVISO (M)SLA from Pujol and Larnicol (2005); hereafter AVISO
- The High Resolution (M)SLA with bathymetric constraint described in Escudier et al. (2013) ; hereafter HR+Bathy

The AVISO fields are a specific product for the Mediterranean Sea, obtained by merging delayed-time "Updated" along track altimetry (SSALTO-DUACS, 2006). They are computed weekly on a 1/8◦ x 1/8◦ Mercator grid. The spatial and temporal correlation scales used to obtain this altimetry fields are, respectively, 100 km and 10 days.

The more recent HR+Bathy fields are computed by interpolating the same along-track altimetry data but by adding smaller spatial and temporal correlation scales in the OI scheme (30 km and 3 days). For the AVISO field the spatial correlation is assumed to be isotropic. However, dynamical structures in the coastal zone are known to be anisotropic due to the strong bathymetry constraint (Liu and Weisberg, 2005). The HR+Bathy fields are thus computed modifying the correlation scales of OI in order to better take into account the shape and propagation of coastal features. The reader specifically interested in the details of the 2D mapping procedures can refer to each of the associated references.

In this study, the AVISO and HR+Bathy (M)SLA are spatially interpolated on a common horizontal grid of 1/8◦ x 1/8◦. The AVISO maps are available only on a weekly basis, whereas the HR+Bathy maps are computed each day. Hence a daily AVISO (M)SLA is created by linear interpolation in time. The daily geostrophic current anomaly fields are then derived by applying the geostrophic balance equation.

2.2 Mean currents

As previously reminded, the long term mean (1993-1999) of the altimeter Sea Surface Height ($\overline{SSH} = \overline{(M)SLA + MDT + Geoid} = MDT + Geoid$) is subtracted from SSH observations to remove the geoid contribution. However, this procedure also removes the contribution due to the MDT. Therefore, mean currents have to be estimated from an independent source and added to the (M)SLA-derived anomaly currents in order to obtain the absolute geostrophic currents. In this paper, two kinds of mean currents specifically computed for the Mediterranean Sea (see Figure 2) are used and evaluated:

- The mean geostrophic currents derived from the MDT of Rio et al. (2007); hereafter Rio07
- The mean geostrophic currents derived from the MDT of Dobricic (2005); hereafter Dobricic05

The standard MDT from Rio et al. (2007) is built from the results of the 1/8◦ x 1/8◦ Mediterranean Forecasting System model (MFS, Pinardi et al., 2003) for the period 1993–

4

1999 (see Figure 2a). The MFS does not directly apply data assimilation. However, this MDT includes corrections from drifter velocities and altimetric SLA. These data are combined together to obtain local estimates of the mean geostrophic circulation. These estimates are then used in an inverse technique to improve the MDT computed from the model (which is used as a first guess).

The MDT from Dobricic (2005) (see Figure 2b) is also estimated from the MFS model for the 1993–1999 periods, but with the assimilation of temperature from XBT observations and altimetric SLA. The MDT computation is mainly based on the assumption that the error in the MDT field appears in the assimilation system as a temporally constant but spatially variable observational bias. This error can thus be reduced by subtracting the long term average of the dynamic topography departures from the MDT first guess.

From Figure 2, it follows that the two mean current fields show maximum intensity along the NC, confirming that this structure is the dominant dynamical feature of the NWMed (refer to section 1). Depending on the considered field, regional differences in terms of current magnitude and direction can however be observed.

Figure 2

2.3 *In situ* data

The 16 drifter trajectories used for validation (see table 1) were launched within the framework of the LAgrangian Transport EXperiments (LATEX) conducted in summer 2008, 2009 and 2010 by the Mediterranean Institute of Oceanography (M.I.O.) in order to study the influence of mesoscale structures on both physics and biochemistry in the western GoL. Each drifter was tethered to a holey-sock drogue centred at 15 m. In 2008 and 2010, the drifters trajectories are exploited in our analysis for a period of 60 days after their launch (T_0), during which the drifters did not strand ashore and remained inside our study area (see Figure 3). In 2009, trajectories were exploited (Figure 3b) for only 20 days, the maximum period of available data, before two of the three drifters launched were lost.

Table 1

Until the present study, altimetry data have not yet been analyzed within the framework of Latex08 and Latex09 campaigns. On the other hand, the near real time AVISO data showed inconsistencies with respect to the drifter trajectories of Latex10, especially close to the GoL coast (Nencioli et al., 2011). Thus, the comparison between altimetry and drifters trajectories from Latex08, Latex09 and Latex10 gives a good opportunity to evaluate the relative performances of new altimetry products in the NWMed.

Figure 3

2.4 Methods of validation

Our method is principally inspired by the one of Liu and Weisberg (2011) initially developed for the evaluation of modeled trajectories over the Gulf of Mexico and successfully applied to the Norway Coast (Röhrs et al., 2012). Here, our main purpose is to diagnose the relative performances of the different combinations of OI scheme (section 2.1) and mean current (section 2.2) for computing absolute geostrophic currents. Our improved method, which aims at computing a Lagrangian skill score, consists of three steps:

1) For each drifter, each day, N virtual particles (336) are launched in a square centered on the drifter initial position (grey squares on Figure 4a, 4b). The square is set to a width of 30 km corresponding to the spatial correlation scale from Escudier et al. (2013). The initial intergrid spacing between each particle is about 1.5 km which is similar to previous Lagrangian-based studies over the Mediterranean Sea (e.g. D'Ovidio et al., 2004; Lehan et al., 2007; Nencioli et al., 2011).

2) Every day, the virtual particles are advected for a given time interval T using each of the 4 altimetry-derived currents (combinations of 2 OI methods and 2 mean currents).The advection scheme is a *fourth-order Runge-Kutta* integrator (see d'Ovidio et al. 2004) with a time-step of 3 hours. The velocities are interpolated bi-linearly in space and linearly in time. The chosen time interval for advection is either T=10 days (temporal correlation scale of the AVISO OI scheme) or T=3 days (temporal correlation scale from Escudier et al., 2013). An illustration is provided on Figure 4 and shows the virtual particle dispersion after 10-day advection.

Figure 4

3) For each particle *p* and drifter *D*, we then compute the normalized cumulative separation distance $s_{D,p}$ defined in Liu and Weisberg (2011) as:

$$s_{D,p}(t,x) = \frac{\sum_{i}^{T} d_i}{\sum_{i}^{T} l_i} \qquad \text{(Eq. 1)}$$

with d_i the distance between the virtual particle *p* and the *in situ* drifter positions and l_i the length of the drifter trajectory after a time *i* of advection from the drifter initial position. $s_{D,p}$ scores are then computed every day t and position x (x,y).The procedure to compute $s_{D,p}$ is repeated each day for all the virtual particles launched around a given drifter *D*. For each drifter *D*, the daily values of $s_{D,p}$ can be averaged together to obtain the mean score $S_D(t,x)$ defined as:

$$S_D(t,x) = \frac{1}{N}\sum_{p=1}^{N} s_{D,p}(t,x) \qquad \text{(Eq. 2)}$$

Among the virtual particles released, only the *N* ones ($N \leq 336$) which are not stranded ashore are used in the average computation (Eq. 2). Based on this definition, the smaller the value of S_D, the more accurate the altimetry absolute velocity field. To avoid any confusion, it is important to note that this score is similar to the "*normalized cumulative separation distance*" defined in Eq.1 in Liu and Weisberg (2011) but generalized to particle clusters (and thus not the “skill score” defined in Eq. 2-3 of the same paper).

The use of particle clusters is preferred over single particles as in Liu and Weisberg (2011) since it ensures more robust statistical results (Shroeder et al., 2012). As expected, experiments using a single synthetic trajectory (N=1) showed noisier results than for an ensemble of synthetic trajectories (N=336) with S_D standard deviations about 20 % higher (with T=10 days for the whole drifters and periods). Several sensitivity tests with different

6

number of particles were performed (not shown since the results did not provide additional information to the present ones). As mentioned before, the number of 336 particles was chosen since it provided an initial particle spacing of the order 1.5 km, in the range of previous studies.

By averaging together the S_D values of each drifter D, it is possible to compute the temporal mean score $\overline{S}_D$ for the period T_0 (60-day mean for Latex08 and Latex10, 20-day mean for Latex09).

$$\overline{S}_D = \frac{1}{T_0}\sum_{t=1}^{T_0} S_D(t,x) \qquad \text{(Eq. 3)}$$

Finally, by computing the average of every drifter we can retrieve $\overline{S}$, the ensemble mean per LATEX experiment.

Figure 5 shows the temporal evolution of $S_{D=1}$ (drifter 1) and $S_{D=9}$ (drifter 9) between September and November 2010 (see Figure 4 for their respective trajectories), in a case where the velocity field products do not show strong S differences (<1). These curves, computed with 3-day and 10-day advection, are mostly used to illustrate the variation of S_D with respect to the time of advection. For a same product, the curves show similar patterns but differences in the amplitude: the longer the time integration, the larger the score. S_D is indeed higher for 10-day advection than for the 3-day. This result, confirmed by experiments done with 60-days advection (not shown), is in agreement with Lagrangian theory and chaotic transport showing that the separation rate between two trajectories will increase exponentially for spatial scales less than the deformation radius (Garrett, 1983) or linearly at greater scales, after 10-60 days advection (Nilsson et al., 2013)

However, the increase of the score with larger T (as observed on Figure 5), depends not only on the accuracy of the velocity field, but also on the local kinematic properties of the flow itself. In other words, since the score is computed using a cluster of particles, for a same time advection T, score differences between two products can be due to their respective accuracy, but also due to the dispersive characteristics of the velocity fields. In order to evaluate the dispersion rate associated with each product, we have computed the local strain rate (γ, see Eq. 4) at all virtual particle positions.

$$\gamma_{D,p}(t,x) = \left(\frac{\partial u}{\partial x} - \frac{\partial v}{\partial y}\right)^2 + \left(\frac{\partial v}{\partial x} + \frac{\partial u}{\partial y}\right)^2 \qquad \text{(Eq.4)}$$

Analogously to Lagrangian diagnostics such as the Finite Time/Size Lyapunov Exponent, the strain rate is an Eulerian diagnostic that quantifies the tendency of the flow field to disperse initially close particle trajectories (e.g. Waugh et al., 2005). The same average procedures done for $s_{D,p}$ are applied to $\gamma_{D,p}$ in order to make the mean strain rate $\overline{\gamma}$ directly comparable with $\overline{S}$ and therefore evaluate the scores of different velocity fields also in the light of their respective dispersion rate.

This point is addressed in section 3.1 by focusing on the 2 altimetric current products which show the most statistically different results. In a second step, statistics are presented regionally, aiming at discriminating the relative influence of mean currents and OI methods (section 3.2).

Figure 5

2. Results

3.1 Comparisons of current fields

2.1.1. Statistics at the basin scale

In this section we focus on the comparison between 2 of the products presented in section 2: The first one (hereafter called *standard*) is the standard regional AVISO gridded field combining standard AVISO (M)SLA with geostrophic mean current derived from Rio07. The second one (hereafter called *new*) is an alternative current field which consists of the combination of geostrophic currents derived from HR+Bathy (M)SLA (Escudier et al., 2013) with the MDT Dobricic05. For the three LATEX experiments (see table 1), the mean strain rate of the *new* product (0,70 day^{-1}) is higher than the *standard* one (0.61 day^{-1}), showing equivalent space-time variations (mean STD differences <8%). Thus, the *new* product is on average slightly more dispersive than the standard one.

The main statistical results obtained at drifters positions are summarized in table 2 and show that the *new* surface gridded field has smaller $\overline{S}$ both with 10- and 3-day advection (less pronounced with 3 days) although its strain rate is higher: the average $\overline{S}$ scores ($\overline{\gamma}$) with 10-day advection for all the drifters and the three LATEX periods is of 4.3 (0.62 day^{-1}) and 3.7 (0.75 day^{-1}) for respectively the *standard* and *new* gridded geostrophic currents. This represents a mean improvement for the *new* product with respect to the *standard* one despite a larger mean strain rate.

When we look at the scatterplots of S and γ values (Fig.6), it appears that there is no clear relation between these two quantities. Indeed, for the *standard* product (Fig.6a) some strong S values (>10, see red square) are associated with low γ (< 0.75 day $^{-1}$) whereas for the *new* product (Fig.6b) some relatively low S values (<5, see blue square) can correspond to high γ (> 1 day $^{-1}$). This means that even if a stronger strain rate tends to increase S by increasing the dispersion rate of the virtual particles, this could be compensated by a more accurate velocity field decreasing the average distance between the drifter and the virtual particles.

Figure 6

Having evidenced that *S* is more representative of the velocity field quality than of its Lagrangian dispersion (especially for high *S* score), we can now analyze in details the trajectories and the associated spatial distribution of S_D for 2 drifters (drifters 4 and 6 of Latex10) showing strong S_D values for a relatively low strain rate (inside the red square of Fig.6a).

2.1.2. Regional differences

Both for drifter 4 and drifter 6, the worst $S_{D=4}$ and $S_{D=6}$ are obtained between the last week of September and the first week of October. This period corresponds to a northward drifter migration not well reproduced by altimetry-derived currents despite results being significantly better with the *new* field (black curves on Fig.7). Indeed, as observed in Nencioli et al. (2011), these two drifters - launched at the same time - are first advected in a shallow coastal area north of the GoL where the circulation dynamics might be partially ageostrophic because of intense wind and/or bathymetric effects. Other than over these particular zones, drifters 4 and 6 show relative low S_D scores (< 4), especially for the *new* fields, when the

8

drifters started to be advected southwards along the coastal corridor identified by Nencioli et al. (2011) in the south-western part of the GoL (see Figure 1).

Figure 7

The analysis of $S_{D=4}$ and $S_{D=6}$ highlights significant differences between the *standard* and *new* satellite-derived velocity fields. We therefore further investigate these differences by analyzing the daily S_D score along all drifter trajectories from the LATEX experiments, and focusing in particular on its spatial distribution. For clarity we only discuss the S_D scores with 10-day advection for Latex10 and Latex08, since they are characterized by longer drifter trajectories (conclusions for Latex09 and with 3 days advection are however similar).

The southern parts of the GoL show relative good statistics with relative small S_D scores (<3 for Latex08 and Latex10) for both *new* (Figure 8 b,e) and *standard* (Figure 8a, 8d) fields (for all drifters/times). This is true even very close to the coast, along the coastal corridor (Figure 1) described in Nencioli et al. (2011) suggesting that the dynamics over this area is quite stable and geostrophic.

Figures 8c and 8f highlight the S_D difference between *standard* and *new* surface gridded currents respectively for 2008 and 2010. Except in the Catalan Sea and near the west Corsica and Sardinia coasts, the *new* fields are characterized by better statistics. The major differences are observed over the GoL continental shelf where the *new* velocity field shows lower S_D (difference > 2) for both Latex08 and Latex10.

In the north-western part of this area, high S_D scores were previously observed for drifter 4 and drifter 6 but not for all the Latex10 drifters reaching this region. There are three possible reasons (or a combination of them): 1) the dynamical structures are maybe too small or close to the coast to be captured by the conventional along-track measurements (instrument limitation); 2) the OI methods smooth a large part of the altimetry signal even with smaller and bathymetry-constrained correlation scales (methodology limitation); 3) Episodic and small-scale ageostrophic dynamics may dominate the surface signals (see introduction and associated references).

Figure 8

Considering all the drifters and all the Latex periods, the mean $\overline{S}$ scores over the GoL is 3.6 against 4.5 for respectively the *new* and *standard* velocity fields. This represents a stronger regional improvement of the *new* product (> 20 %) with respect to result obtained over the entire NWMed domain (~15%, see section 3.1.1). S_D along the continental shelf slope is relatively good (<3), especially for Latex 2008. There, stable dynamical features may be influenced by bathymetry and altimetry appears to be well adapted to resolve the associated geostrophic dynamics. This seems not to be always the case in shallower regions in the north-western part of the GoL, as observed during the Latex10 experiment. In order to address this issue, we now focus on a specifics event occurring at the beginning of Latex08.

2.1.3. *Focus on a coastal eddy*

Numerous numerical simulations and analysis of multi-source data from Latex08 and Latex09 have already identified the recurrent presence in summer of an intense anticyclonic eddy of about 20 km radius in the western side of the GoL (Hu et al, 2009; Kersalé et al.,

9

2013). It is clearly depicted in drifter trajectories of Figure 3a and Figure 3b. In 2001, one such eddy was also modeled both physically (Hu et al., 2011) and biogeochemically (Campbell et al., 2012). The issue addressed here is to check if altimetry gridded fields are able to reproduce or not this coastal mesoscale feature

For this, 336 virtual particles are launched in the 15 km neighborhood of the initial positions of the 2 drifters trapped by the eddy of Latex08. Then, the particles are advected for 10 days both with the *standard* and the *new* absolute geostrophic velocities and compared qualitatively to real drifters trajectories. From Figure 9 it turns out that most of the particles advected by the *new* field (Figure 9b) roughly follow the drifter positions (corresponding to low *S* scores), even if the location of the physical structure seems to be partially inaccurate. Concerning the *standard* AVISO currents (Figure 9a), all the particles go directly southward, without following the observed eddy loop (corresponding to high *S* scores).

Analysis of this event proves that the *new* field, using a bathymetric constraint and the Dobricic05 mean current, better represents well developed, stable, coastal geostrophic mesoscale features such as the one observed during Latex08. A similar conclusion is found by Escudier et al. (2013) by comparing drifter-derived currents, glider and altimetry north of Mallorca with Eulerian approaches. However, for Latex09 (not shown) neither the *new* nor the *standard* velocity field are able to reproduce such an eddy-like structure. This structure is too small and/or too close to the coast to be captured with conventional altimetry or reproduced by the 2D fields, even by the use of innovative OI techniques and alternative MDT.

Figure 9

3.2 Influence of mean currents and optimal interpolation methods

3.2.1 *Statistics at the basin scale*

The previous results have pointed out significant differences between *new* and *standard* gridded fields both qualitatively and quantitatively. However, they did not inform on the respective influence of OI methods (see section 2.1) and mean currents (see section 2.2) on the Lagrangian metrics. In order to isolate the relative influence of OIs (respectively mean currents), we compute, for each OI (respectively mean currents), the average of the two $\overline{S}$ scores using the two available mean currents (respectively OIs). Table 3 shows the average $\overline{S}$ score for the different OI methods. Both with 10-day and 3-day advection, the mean $\overline{S}$ score are very close and do not allow to conclude whether one OI approach is better than another. From table 3, it however turns out that the mean current from Dobricic05 exhibits better statistics than the Rio07 one (~12 % of improvement with 10-days advection)..

Table 3

This shows that mean currents have a stronger influence than the OI methods on our Lagrangian diagnostics. However, even if this is true at the NWMed Basin scale, alternative OI methods might still have significant regional impacts, especially in shallow areas where the smaller correlation scale and bathymetric constraints described by Escudier et al. (2013) may have stronger impacts.

10

3.2.2 Focus on the Gulf of Lion

We now focus on the GoL area where major differences, both quantitative and qualitative, between the *new* and *standard* product were previously observed. In order to assess the influence of the bathymetry constraint in the Lagrangian statistics, we compute the $\overline{S}$ score for three bathymetric classes (Figure 10 right). The $\overline{S}$ score is only computed if at least 10 drifter positions are available for a given bathymetric class. Except for 2009, the number of positions is between 20 and 100, depending on the time of advection and of the LATEX mission.

Figure 10

For Latex08 (Figure 10a) and Latex09 (10b), the two OI methods show similar statistics for any of the considered bathymetric classes, despite the qualitative differences evidenced in section 3.1.3. Concerning the mean current, the scores are quite similar for depth <150 m (S~3.0 for 10-day advection); but for the other bathymetric classes; Dobricic05 exhibits better score than Rio07. It is also somehow surprising to note that the score in 2008 and 2009 are generally better in shallow water areas of the GoL (S~3 for depth < 150 m) than in deeper zones (S~4 for depth>150 m) where potential small scale and partially ageostrophic instabilities may arise close to the NC external borders. This confirms that circulation over the GoL continental shelf during these two cruises is in good geostrophic balance and is relatively well resolved by altimetry gridded fields.

For Latex10 (Figure 10 c, f) the conclusions are quite different. In that case, the different OI methods exhibit significant differences for depth less than 150 m (located North West of the GoL). By comparison with the AVISO $\overline{S}$ score with 10-day (3-day) advection, HR+Bathy shows improvements of 13 % (23%) whereas less pronounced differences are observed depending on the considered mean currents. This indicates that the new OI method can have significant impact for some specific events in shallow-water regions. In our case, this corresponds to smaller scale dynamics influenced by the bathymetry that trapped and retained drifters close to the coast. Concerning the mean currents, Dobricic05 have again smaller $\overline{S}$ for the whole bathymetric classes confirming the conclusion obtained for Latex08 and Latex09.

3. Discussions and conclusions

Cross-shelf exchanges are of crucial importance to study the impact of anthropogenic discharged pollutants, oil spill as well as the transport of natural biogeochemical elements and biological organisms (e.g. nutrients, larvae, jellyfishes). A quantitative understanding of coastal physical processes and associated Lagrangian transport is therefore necessary to determine how the ocean dynamics affects the biological and ecological conditions of coastal environments.

In this paper, new absolute geostrophic currents, derived from satellite altimetry observations in combination with models are processed and evaluated using a Lagrangian diagnostic based on particle cluster advection. In agreement with the finding of Escudier et al. (2013) - based on Eulerian diagnostics- our Lagrangian approaches demonstrate that the use of HR+Bathy (M)SLA generally gives a better representation of transport patterns over the continental shelf (despite still evidencing some inaccuracies/limitations in the positioning of small scale structures). In addition, we have also demonstrated that the use of an alternative

 11

mean current (ie from Dobricic 2005) rather than the standard one (ie Rio et al., 2007) significantly improves the comparison with drifter trajectories, especially along the corridor located at the south west Gulf of Lion.

However, the relatively limited *in situ* dataset used in our study did not allow for more extensive Lagrangian statistical analysis requiring to compare cluster of particle trajectories with a larger number of drifters. As a perspective, it would be relevant to adopt our approach with all the available drifters in the Mediterranean Sea (> 500 trajectories sine 1992, Poulain et al., 2012a). This should allow the generation of a more complete and robust altimetric error map over the Mediterranean Sea than the ones obtained during the three LATEX experiments. In a second step, the whole drifter database could also be exploited in synergy with altimetry and modeling (with assimilation schemes or statistic constraints) in order to generate a new and more accurate regional Mean Dynamic Topography for coastal applications.

Concerning the Optimal Interpolation methods, the use of shorter and bathymetric constrained correlation scales is not always sufficient to significantly improve the statistics over the whole North Western Mediterranean. However, we pointed out that in some specific cases and areas, such as the continental shelf in the western part of the Gulf of Lion, improvements can be obtained (as also observed in the Balearic Sea by Escudier et al., 2013). However, the relative sparse space/time coverage of existing along track altimetric missions (such as during the 2008-2010 period) is a clear limitation for the long-term tracking and analysis of small-scale dynamics even through the development of coastal-oriented Optimal Interpolation methods. Coastal altimetry will undoubtedly benefit, in the near future, of a denser satellite constellation and new altimetry sensors. Waiting for SWOT satellite (Fu and Ferrari, 2012), Lagrangian studies of coastal mesoscale dynamics will thus require the integration of data from the Saral/AltiKa and Cryosat-2 missions in the Optimal Interpolation schemes.

Our statistical Lagrangian analyses are in agreement with qualitative considerations and previous Eulerian studies over the North Western Mediterranean Sea. However, further investigations should be done in order to better discriminate the relative contribution to the *S* score due to the influence of dispersive effects (related to the strain rate) and due to the intrinsic accuracy of the velocity field. Another critical aspect concerns ageostrophic motions which could influence the transport of tracers in the surface layer but that are not included in altimetry. Their impacts -not addressed in this study - may be more important in coastal zones and could be therefore at the base of significant observed discrepancies between drifter and altimetric trajectories. For example, Liu and Weisberg (2007) show, over the Florida shelf, that the across-shelf wind effects (ageostrophic part) are secondary compared to the barotropic geostrophic currents but can be stronger than the baroclinic ones.

The relation between surface and sub-surface mesoscale is also a challenging issue requiring both the continuous development of theoretical models and high resolution 2D gridded current (Dussurget et al., 2011, Gaultier et al., 2013; Escudier al., 2013). Our Lagrangian diagnostics applied to sub-surface drifters could also be used in a near future in order to compare results obtained from different reconstructions methods (e.g. Carnes et al, 1994; Lapeyre and Klein, 2006; LaCasce and Mahadevan, 2006; Scott and Furnival 2012). The use of 3D observation-based currents associated with Lagrangian tools is promising and might pave the way to new ecological applications for coastal altimetry such as the influence cross-shelf exchanges on fish larvae, plankton or transport and landing over the north western Mediterranean coastal domain

References

12

Anzenhofer, M., Shum, C.K., Rentsh, M. Coastal altimetry and applications, Tech. Rep., 464, Geod. Sci. and Survey, Ohio State University, Columbus, 1999

Birol, F., Cancet, M., Estournel, C. Aspects of the seasonal variability of the Northern Current (NW Mediterranean Sea) observed by altimetry, J. Mar. Syst., 81, 297–311, 2010. doi:10.1016/j.jmarsys.2010.01.005.

Bouffard, J., Roblou, L., Birol, F., Pascual, A., Fenoglio-Marc, L., Cancet, M., Morrow, R., Ménard, Y. Introduction and assessment of improved coastal altimetry strategies: case study over the North Western Mediterranean Sea. Chapter 12 in S. Vignudelli, A.G. Kostianoy, P. Cipollini, J. Benveniste (eds.), Coastal Altimetry, Springer-Verlag Berlin Heidelberg, 578 pp, 2011. DOI: 10.1007/978-3-642-12796-0_12

Bouffard, J., Renault, L., Ruiz, S., Pascual, A., Dufau, C., Tintoré, J. Sub-surface small scale eddy dynamics from multi-sensor observations and modelling, Progress In Oceanography, vol. 106, 62-79, 2012.

Bouffard, J., Vignudelli, S., Cipollini, P., Ménard, Y. Exploiting the potential of an improved multi-mission altimetric dataset over the coastal ocean. Geophysical Research Letter (GRL), 35, 2008b. DOI:10.1029/2008GL033488.

Bouffard, J., Vignudelli, S., Hermann, M., Lyard, F., Marsaleix, P., Ménard, Y., Cipollini P. Comparison of ocean dynamics with a regional circulation model and improved altimetry in the Northwestern Mediterranean. Journal of Terr. Atm.. and Oceanic Sciences, 19, No 1-2, 117-133, 2008a. DOI: 10.3319/TAO.2008.19.1-2.117(SA).

Bouffard, J., Pascual, A., Ruiz, S., Faugère, Y., Tintoré, J. Coastal and mesoscale dynamics characterization using altimetry and gliders: A case study in the Balearic Sea, J. Geophys. Res., 115, C10029, 2010. doi:10.1029/2009JC006087.

Campbell, R., Diaz, F., Hu, Z.Y., Doglioli, A.M., Petrenko, A.A., Dekeyser, I. Nutrients and plankton spatial distributions induced by a coastal eddy in the Gulf of Lion. Insights from a numerical model, Progress in Oceanography, 2012. doi: 10.1016/j.pocean.2012.09.005.

Carnes, M.R., Teague,W.J., Mitchell, J.L. Inference of subsurface thermohaline structure from fields measurable by satellite, J. Atmos. Ocean. Tech., 11, 551–566, 1994.

D'Ovidio, F., Taillandier, V., Taupier-Letage, I., Mortier, L. Lagrangian validation of the Mediterranean Mean Dynamic Topography by extraction of Tracer Frontal Structures, Newsletter Mercator #32 : The Mediterranean Sea. 2011.

D'Ovidio, F., Fernandez, V., Hernandez-Gracıa, E., Lopez, C. Mixing structures in the Mediterranean Sea from finite-size Lyapunov exponents, Geophys. Res. Lett., 31, 2004. doi:10.1029/2004GL020328

Dobricic, S. New mean dynamic topography of the Mediterranean calculated from assimilation system diagnostics, Geophys. Res. Lett., 32, 2005. doi:10.1029/2005GL022518

Dussurget, R., Birol, F., Morrow, R., De Mey, P. Fine Resolution Altimetry Data for a Regional Application in the Bay of Biscay, Marine Geodesy, 34:3-4, 447-476, 2011. http://dx.doi.org/10.1080/01490419.2011.584835

Escudier, R., Bouffard, J., Pascual, A. Poulain, P.-M. Improvement of coastal mesoscale observation from space: Application to the North Western Mediterranean, Geophys. Res. Letter,40, Issue 10, 2148–2153, 2013. DOI: 10.1002/grl.50324

13

Fu, L.-L., Chelton, D.B. Large-scale ocean circulation. In: Satellite Altimetry and Earth Sciences: A Handbook for Techniques and Applications. Academic Press, San Diego, edited by L.-L. Fu and A. Cazenave, 423, 133-16, 2001.

Fu, L.-L., Ferrari, R. Observing oceanic submesoscale processes from space. Eos, Transactions, American Geophysical Union 89(48):488, 2008.

Fu, L.-L., Chelton, D.B., Le Traon, P.-Y., Morrow, R. Eddy dynamics from satellite altimetry. Oceanography 23(4):14–25, 2010. http://dx.doi.org/10.5670/oceanog.2010.02.

Garrett, C. On the initial streakiness of a dispersing tracer in two– and three– dimensional turbulence. Dynamics of Atmospheres and Oceans, 7, 265–277. 1983

Gatti, J. Intrusions du Courant Nord Méditerranéen sur la partie est du plateau continental du Golfe du Lion , thèse de doctorat de l’Université de Provence (PhD Thesis in french), soutenue le 16/06/2008 à Marseille, 2008.

Gaultier, L., Verron, J., Brankart, J.-M., Titaud, O., Brasseur, P. On the inversion of submesoscale tracer fields to estimate the surface ocean circulation. Journal of Marine Systems, 126, 33-42, 2013. http://dx.doi.org/10.1016/j.jmarsys.2012.02.014

Gostan, J. Etude du courant géostrophique entre Villefranche-sur-Mer et Calvi. Cahiers océanographiques XIXme année - Service Hydrographique de la Marine, 4, 329-345. 1967.

Hu, Z.Y., Doglioli, A.M., Petrenko, A.A., Marsaleix, P., Dekeyser, I. Numerical simulations of eddies in the Gulf of Lion. Ocean Modelling, 28, 203-208, 2009. http://dx.doi.org/10.1016/j.ocemod.2009.02.004

Hu, Z.Y., Petrenko, A.A., Doglioli, A.M., Dekeyser, I. Numerical study of eddy generation in the western part of the Gulf of Lion. J. Geophys. Res., 116, C12030, 2011. doi:10.1029/2011JC007074.

Huthnance, J.M. Circulation exchange and water masses at the ocean margin. Progress in Oceanography, 35, 353-431. 1995

Kersalé, M., Petrenko, A.A., Doglioli, A.M., Dekeyser, I., Nencioli. F. Physical characteristics and dynamics of the coastal Latex09 Eddy derived from in situ data and numerical modeling., J. Geophys. Res., 118, 399-409, 2013. doi:10.1029/2012JC008229

Lapeyre, G., Klein, P. Dynamics of the upper oceanic layers in terms of surface quasigeostrophy theory.. J. Phys. Oceanogr., 36, 165–176, 2006.

LaCasce, J., Mahadevan, A., Estimating subsurface horizontal and vertical velocities from sea surface temperature. J. Mar. Res., 64, 695–721, 2006.

Le Traon, P.-Y., Dibarbourne, G. An illustration Of the Contribution of the Topex/Poseidon – Jason-1 Tandem Mission to Mesoscale Variability Studies. Marine Geodesy, 27, 3-13, 2004.

Le Traon, P.-Y. and Dibarboure, G. Mesoscale Mapping Capabilities of Multiple-Satellite Altimeter Missions. J. Atmos. Oceanic Technol., 16, 1208–1223, 1999. doi: http://dx.doi.org/10.1175/1520-0426(1999)016

Liu, Y., Weisberg, R.H. Evaluation of trajectory modeling in different dynamic regions using normalized cumulative Lagrangian separation, J. Geophys. Res., 116, C09013, 2011. doi:10.1029/2010JC006837.

Liu, Y., Weisberg, R.H. Ocean currents and sea surface heights estimated across the west Florida shelf. J. Phys. Oceanogr., 37, 1697–1713, 2007.

 14

Liu, Y., Weisberg, R.H. Patterns of ocean current variability on the West Florida Shelf using the self-organizing map, J. Geophys. Res., 110, C06003, 2005. doi:10.1029/2004JC002786

McGillicuddy, D.J., Anderson, L.A., Bates, N.R., Biddy, T.S., Buesseler, K.O., Carlson, C.A., Davis, C.S., Ewart, C., Falkowski, P.G., Goldthwait, S.A., Hansell, D.A., Jenkins, W.J., Johnson, R., Kosnyrev, V.K., Ledwell, J.R., Li, Q.P., Siegel, D.A. and Steinberg, D.K. Eddy/wind interactions stimulate extraordinary mid-ocean plankton blooms. Science, 316: 1021-1026, 2007.

Millot, C. The Gulf of Lions' hydrodynamics. Continental Shelf Research, 10(9-11), 885-894, 1990.

Millot, C. Mesoscale and seasonal variabilities of the circulation in the Western Mediterranean. Dynamics of Atmospheres and Oceans, 15, 179-214, 1991.

Nencioli, F., d'Ovidio, F., Doglioli, A.M., Petrenko, A.A. Surface coastal circulation patterns by in situ detection of Lagrangian coherent structures, Geophys. Res. Lett., 38, L17604, 2011. doi:10.1029/2011GL048815.

Nilsson, J. A. U., Döös, K., Ruti, P.M., Artale, V., Coward, A., Brodeau, L. Observed and Modeled Global Ocean Turbulence Regimes as Deduced from Surface Trajectory Data. J. Phys. Oceanogr., 43, 2249–2269, 2013. doi: http://dx.doi.org/10.1175/JPO-D-12-0193.1

Pascual, A., Ruiz, S., Tintoré, J. Combining new and conventional sensors to study the Balearic Current, Sea Technology, 51(7), 32-36, 2010.

Petrenko, A.A., Dufau, C., Estournel, C. Barotropic eastward currents in the western Gulf of Lion, north-western Mediterranean Sea, during stratified conditions. J. Marine Syst., 74 (1-2), 406-428, 2008. doi:10.1016/j.jmarsys.2008.03.004

Petrenko, A.A., Leredde, Y., Marsaleix, P. Circulation in a stratified and wind-forced Gulf of Lions, NW Mediterranean Sea: in situ and modeling data. Continental Shelf Research. 25, 7-27, 2005. doi:10.1016/j.csr.2004.09.004

Petrenko, A.A. Circulation features in the Gulf of Lions, NW Mediterranean Sea; importance of inertial currents. Oceanol. Acta, 26, 323-338, 2003.

Pinardi, N., Allen, I., De Mey, P., Korres, G., Lascaratos, A., Le Traon, P.-Y., Maillard, C., Manzella, G., Tziavos, C. The Mediterranean Ocean Forecasting System: first phase of implementation (1998-2001). Ann. Geophys., 21, 1, 3-20, 2003.

Poulain, P.-M., Menna, M., Mauri, E. Surface geostrophic circulation of the Mediterranean Sea derived from drifter and satellite altimeter data. *J. Phys. Oceanogr.*, 42, 973–990, 2012a. doi: http://dx.doi.org/10.1175/JPO-D-11-0159.1

Poulain, P.-M., Gerin, R., Rixen, M., Zanasca, P., Teixeira, J., Griffa, A., Molcard, A., De Marte, M., Pinardi, N. Aspects of the surface circulation in the Liguro-Provençal basin and Gulf of Lion as observed by satellite-tracked drifters (2007-2009). Bollettino di Geofisica Teorica ed Applicata, 53(2):261-279, 2012b.

Pujol, M.-I., Larnicol, G. Mediterranean Sea eddy kinetic energy variability from 11 years of altimetric data, J. Mar. Syst., 58, 121–142, 2005. doi:10.1016/j.jmarsys.2005.07.005.

Rio, M.-H., Poulain, P.-M., Pascual, A., Mauri, E., Larnicol, G., Santoleri, R. A mean dynamic topography of the Mediterranean Sea computed from altimetric data, in situ

 15

measurements and a general circulation model, J. Mar. Syst., 65, 484–508, 2007. doi:10.1016/j.jmarsys.2005.02.006.

Röhrs, J., Christensen, K.H., Hole, L.B., Broström, G., Drivdal, M., Sundby, S. Observation-based evaluation of surface wave effects on currents and trajectory forecasts, Ocean Dynamics, 62, 10-12, 1519, 2012. doi: 10.1007/s10236-012-0576-y

Schroeder, K., Chiggiato, J., Haza, A.C., Griffa, A., Özgökmen, T.M., Zanasca, P., Molcard, A., Borghini, M., Poulain, P.-M., Gerin, R., Zambianchi, E., Falco, P., Trees, C.A. Targeted Lagrangian sampling of submesoscale dispersion at a coastal frontal zone. Geophys. Res. Letters, 39, L1608, 6PP, 2012. doi:10.1029/2012GL051879.

Scott, R. B., Furnival, D.G. Assessment of traditional and new eigenfunction bases applied to extrapolation of sur- face geostrophic current time series to below the surface in an idealizedprimitiveequation simulation. J. Phys. Oceanogr., 42, 165–178, 2012.

SSALTO-DUACS. Ssalto/Duacs user handbook: (M)SLA and (M)ADT near-real-time and delayed-time products, Rep. SALP-MU-P-EA-21065-CLS, Aviso, Ramonville Saint Agne, France, 2006.

Strub, T. High-Resolution Ocean Topography Science Requirements for Coastal Studies, in the Report of the High-resolution Ocean Topography Science Working Group meeting, edited by D. B. Chelton, Ref. 2001-4, College of Oceanic and Atmospheric Sciences, Oregon State University, Corvallis, OR, 224pp, 2001.

Vignudelli, S., Cipollini, P., Reseghetti, F., Fusco, G., Gasparini, G.P., Manzella G.M.R. Comparison between XBT data and TOPEX/Poseidon satellite altimetry in the Ligurian-Tyrrhenian area. Annales Geophysicae, 21(1, Part 1), 123-135, 2003.

Vignudelli, S., Cipollini, P., Roblou, L., Lyard, F., Gasparini, G.P., Manzella, G.M.R., Astraldi, M. Improved satellite altimetry in coastal systems: Case study of the Corsica Channel (Mediterranean Sea). Geophys. Res. Let., 32, L07608, 2005. doi:1029/2005GL22602.

Vignudelli, S., Kostianoy, A., Cipollini, P., Benveniste, J., (eds.). Coastal Altimetry, Springer, 1st Edition., 2011, XII, 566 p. 216 illus., 2011. doi: 10.1007/978-3-642-12796-0.

Waugh, D.W., Abraham, E.R., Bowen, M.M. Spatial variations of stirring in the surface ocean: A case study of the Tasman Sea, J. Phys. Oceanogr., 36, 526-542, 2006.

Aknowledgments: The LATEX project is supported by the programs LEFE/IDAO and LEFE/CYBER of the INSU -Institut National des Sciences de l'Univers - and by the Region PACA -Provence Alpes Côte dAzur. The altimeter (M)SLA were produced by SSALTO/DUACS and distributed by AVISO with support from CNES –Centre National d'Etude Spatiale. We particularly thank Milena Menna (OGS, Trieste, Italy) for processing and providing edited drifter data used within this study. The authors also acknowledge, B. Buongiorno Nardelli, M. Kersalé and R. Campbell for precious comments and useful discussions. Francesco Nencioli acknowledges support from the FP7 Marie Curie Actions of the European Commission, via the Intra-European Fellowship (FP7-PEOPLE-IEF-2011), project "Lyapunov Analysis in the COaSTal Environment" (LACOSTE-299834). Jérôme Bouffard is financed by a CNES post-doctoral grant.

 16

Figure Captions

Figure 1 – Bathymetry (in m) and main surface circulation patterns of the study area. The dashed black arrows correspond to mesoscale currents throughout the year whereas the blue arrows correspond to average well known flow patterns. The coastal corridor is the one characterized by Nencioli et al (2011)

Figure 2 – Mean geostrophic current (module in cm/s) derived from the Mean Dynamic Topography of (a) Dobricic05 and of (b) Rio07 (the current intensity is in cm/s)

Figure 3 - Trajectories of drifters of (a) Latex08, (b) Latex09 and (c) Latex10. The color corresponds to the time of advection since the positions of origin (in day). The white square corresponds to the drifter initial positions.

Figure 4 – Two examples ((a) Drifter 1 and (b) Drifter 9) of Latex10 drifter trajectories (in blue) versus virtual particle advected during 10 days by gridded currents using HR+Bathy (MSLA) and Dobricic (2005) mean current (in red). For more visibility, the daily particle initial positions (in grey squares) and the associated trajectories (in red) are sub-sampled every 5 days along the drifter positions.

Figure 5 - Examples of time evolution of S_D scores for the 4 velocity fields along the Latex10 drifter 1 and drifter 9 with 3 days ((a); (c)) and 10 days advection ((b); (d))

Figure 6 - Scatterplots of S_D vs γ_D (black dots) for the 10 drifters of Latex10 and of $s_{D,p}$ vs $\gamma_{D,p}$ (grey dots) for the whole corresponding particles *p*. (a) *Standard* product (b) *New* product

Figure 7 - Trajectories of drifters (a) 4 and (b) 6 and corresponding S_D time series (respectively (d);(e)) for the *new* - black curves - and *standard* -pink curves - altimetric products for 10 days advection-. In grey are highlighted areas (left) and corresponding periods (right) of bad S_D score

Figure 8 - Spatial distribution of S_D scores (10 days advection) along drifter daily positions for the *standard* ((a) and (d)) and *new* product ((b) and (e)) during Latex08 and Latex10. Spatial distribution of S_D differences between *standard* and *new* products for (c) Latex08 and (f) Latex10. By convention we choose each initial days of advection as drifter daily positions.

Figure 9 – Latex08 drifter trajectories (cyan, green and blue). Two drifters are trapped by the Latex eddy (in green and blue). In red are the virtual particles initially launched at drifters' trapped initial positions and 10 days advected by (a) the *standard* and (b) *new* altimetric current field. In grey are the particles trajectories for the last day of advection.

 17

Figure 10 – (Right) Daily drifter positions used in the bathymetric classes for Latex08; Latex09 and Latex10. In pink are the points located at depths less than 150 m, in cyan the points between 150 m and 2000 m and in green the points at depths higher than 2000 m. (Left). Diagram of mean $\overline{S}$ scores with respect to Latex drifters (a, b, c) for each OI methods and (d, e, f) for each mean currents function of bathymetric classes. The large (respectively thin) diagrams correspond to $\overline{S}$ score with 10 days (respectively 3 days) advection.

18

Revised tables

	Drogue depth (m)	Number	Period of launching	Initial position	Maximum duration (days)
LATEX 2008 (Figure 3a)	15 (~surface)	3	September 01-05 2010	Western GoL	60
LATEX 2009 (Figure 3b)	15 (~surface)	3	August 26-28 2009	Western GoL	20
LATEX 2010 (Figure 3c)	15 (~surface)	10	September 11-24 2008	Western and southern GoL	60

Table 1 - Main characteristics of LATEX drifters

Years / Altimetry Product	2008		2009		2010	
	$\overline{S}$	$\overline{\gamma}$	$\overline{S}$	$\overline{\gamma}$	$\overline{S}$	$\overline{\gamma}$
STANDARD: AVISO + RIO07	3.8 (2.1)	0,64 (0,68)	4.7 (2.0)	0.49 (0,65)	4.5 (2.5)	0,74 (0,70)
***NEW*: HR+BATHY + DOBRICIC05**	**<u>3.6 (2.0)</u>**	0,80 (0,84)	**3.7 (1.9)**	0.80 (0,74)	**<u>3.9 (2.1)</u>**	0,64 (0,64)

Table 2 - Mean $\overline{S}$ scores and $\overline{\gamma}$ (day^{-1}) score for LATEX drifters after 10 days (top) and 3 days (bottom in bracket) of advection with surface altimetric currents. Best $\overline{S}$ scores are in bold and underlined.

Years / Altimetry Product	2008	2009	2010
AVISO OI	3.7 (2.1)	4.6 (2.0)	4.0 (2.1)
HR-BATHY	3.7 (2.1)	4.6 (2.0)	3.9 (2.1)
Rio07	3.8 (2.2)	5.2 (2.1)	4.1 (2.1)
Dobricic05	3.6 (2.0)	4.0 (2.0)	3.8 (2.1)

Table 3 - Mean $\overline{S}$ scores per OI method (averages done with the two mean currents: Rio07 and Dobricic05) and per mean current (average done with the two OI methods: AVISO and HR+BATHY) after 10 (3) day advections

Revised Figures

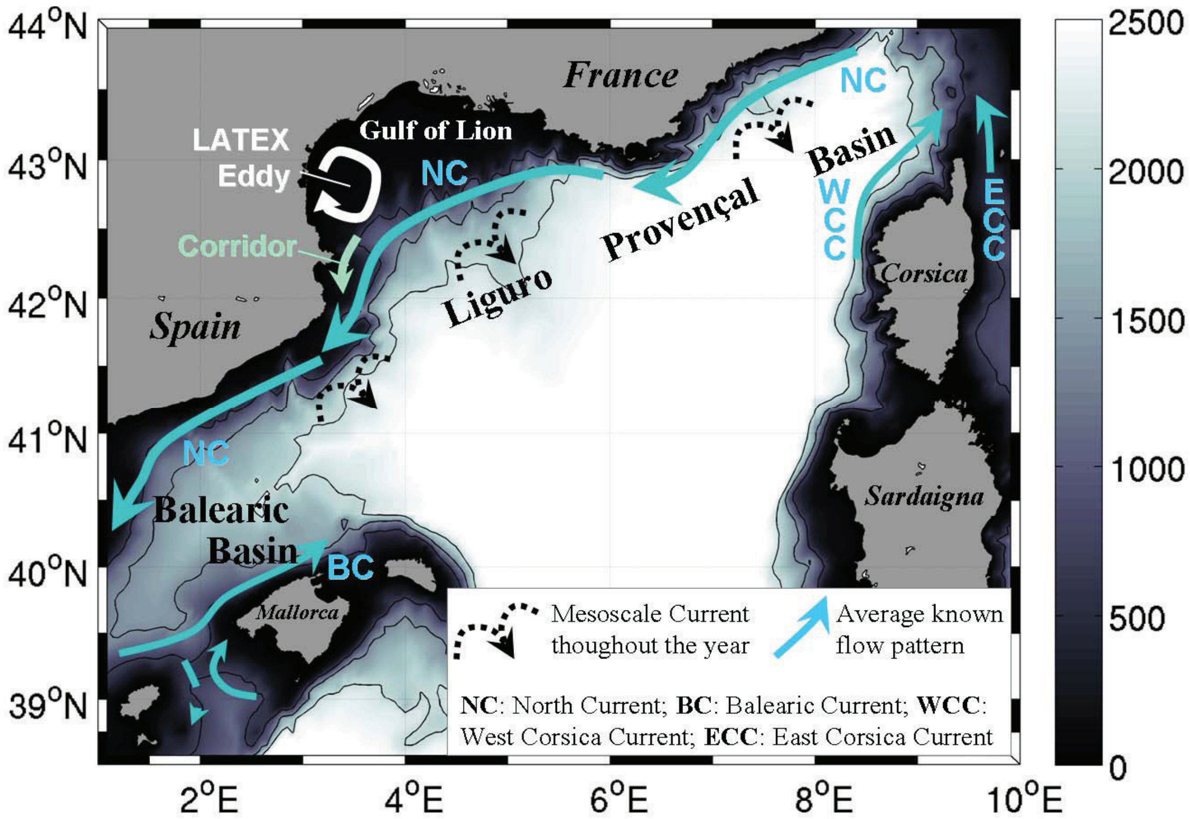

Figure 1 – Bathymetry (in m) and main surface circulation patterns of the study area. The dashed black arrows correspond to mesoscale currents throughout the year whereas the blue arrows correspond to average well known flow patterns. The coastal corridor is the one characterized by Nencioli et al (2011).

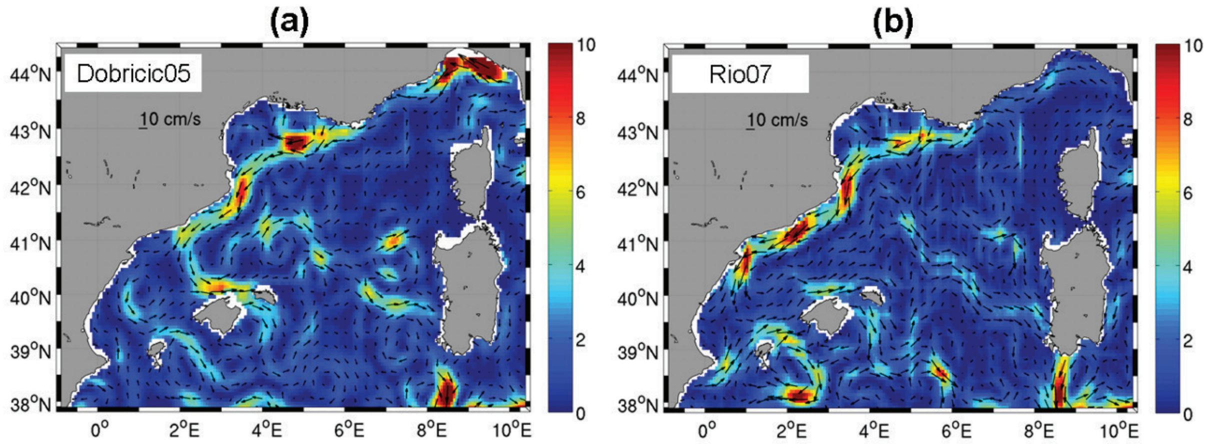

Figure 2 – Mean geostrophic current (module in cm/s) derived from the Mean Dynamic Topography of (a) Dobricic05 and of (b) Rio07 (the current intensity is in cm/s).

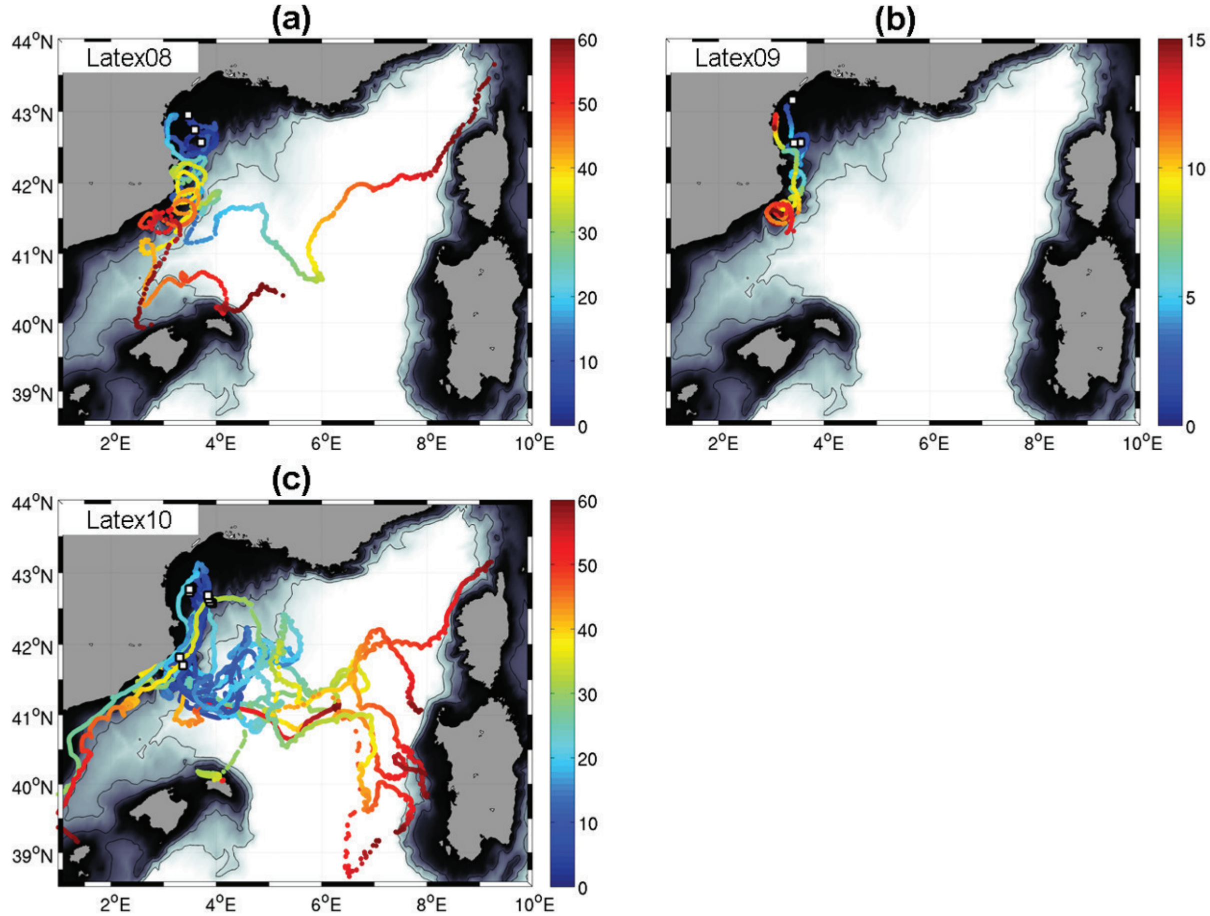

Figure 3 - Trajectories of drifters of (a) Latex08, (b) Latex09 and (c) Latex10. The color corresponds to the time of advection since the positions of origin (in days). The white square corresponds to the drifter initial positions.

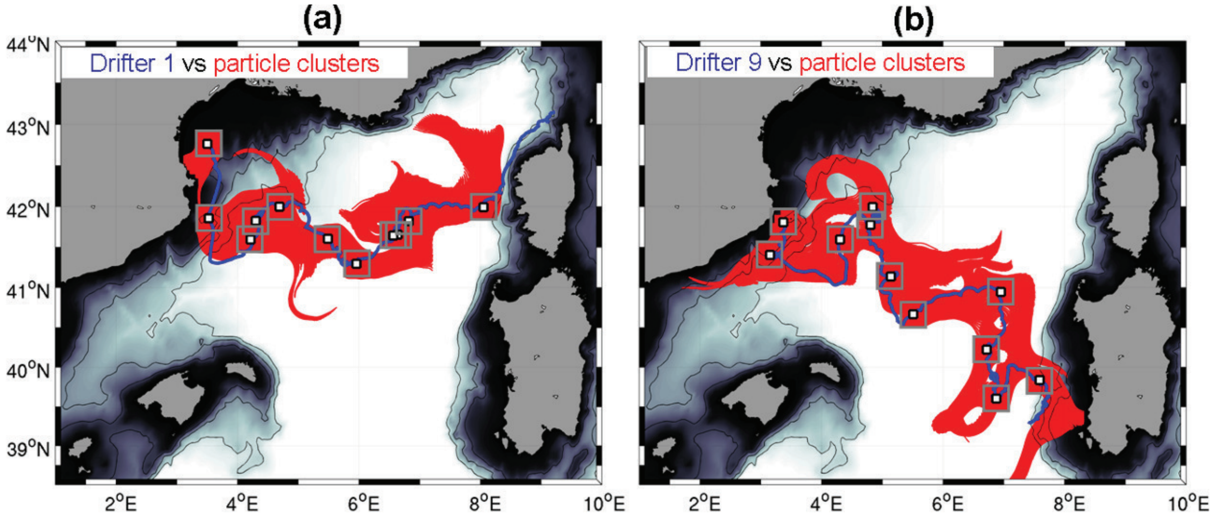

Figure 4 – Two examples ((a) Drifter 1 and (b) Drifter 9) of Latex10 drifter trajectories (in blue) versus virtual particle advected during 10 days by gridded currents using HR+Bathy (MSLA) and Dobricic (2005) mean current (in red). For more visibility, the daily particle initial positions (in grey squares) and the associated trajectories (in red) are sub-sampled every 5 days along the drifter positions.

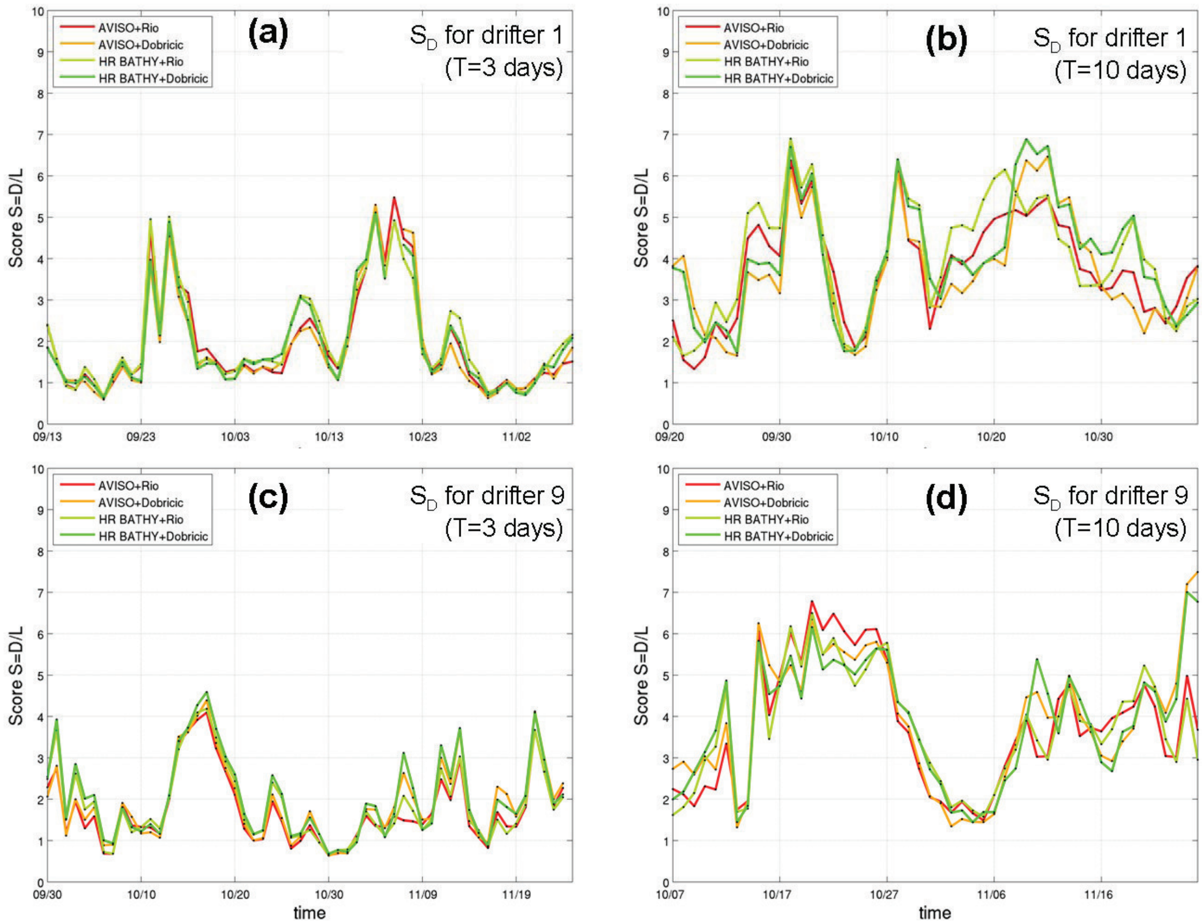

Figure 5 - Examples of time evolution of S_D scores for the 4 velocity fields along the Latex10 drifter 1 and drifter 9 with 3 days ((a); (c)) and 10 days advection ((b); (d))

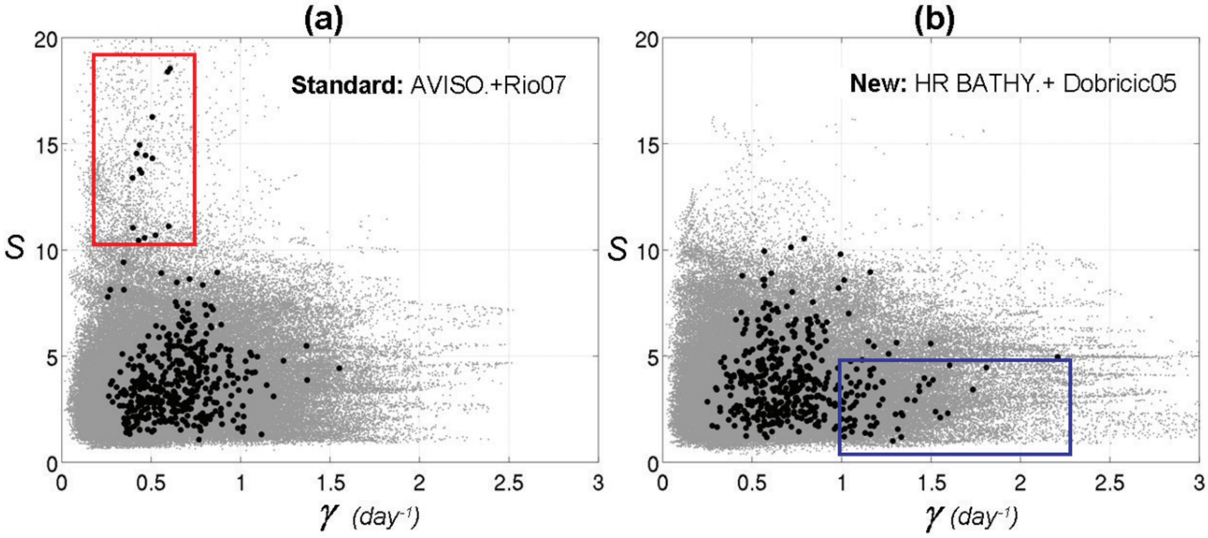

Figure 6 - Scatterplots of S_D vs γ_D (black dots) for the 10 drifters of Latex10 and of $s_{D,p}$ vs $\gamma_{D,p}$ (grey dots) for the whole corresponding particles p. (a) *Standard* product (b) *New* product

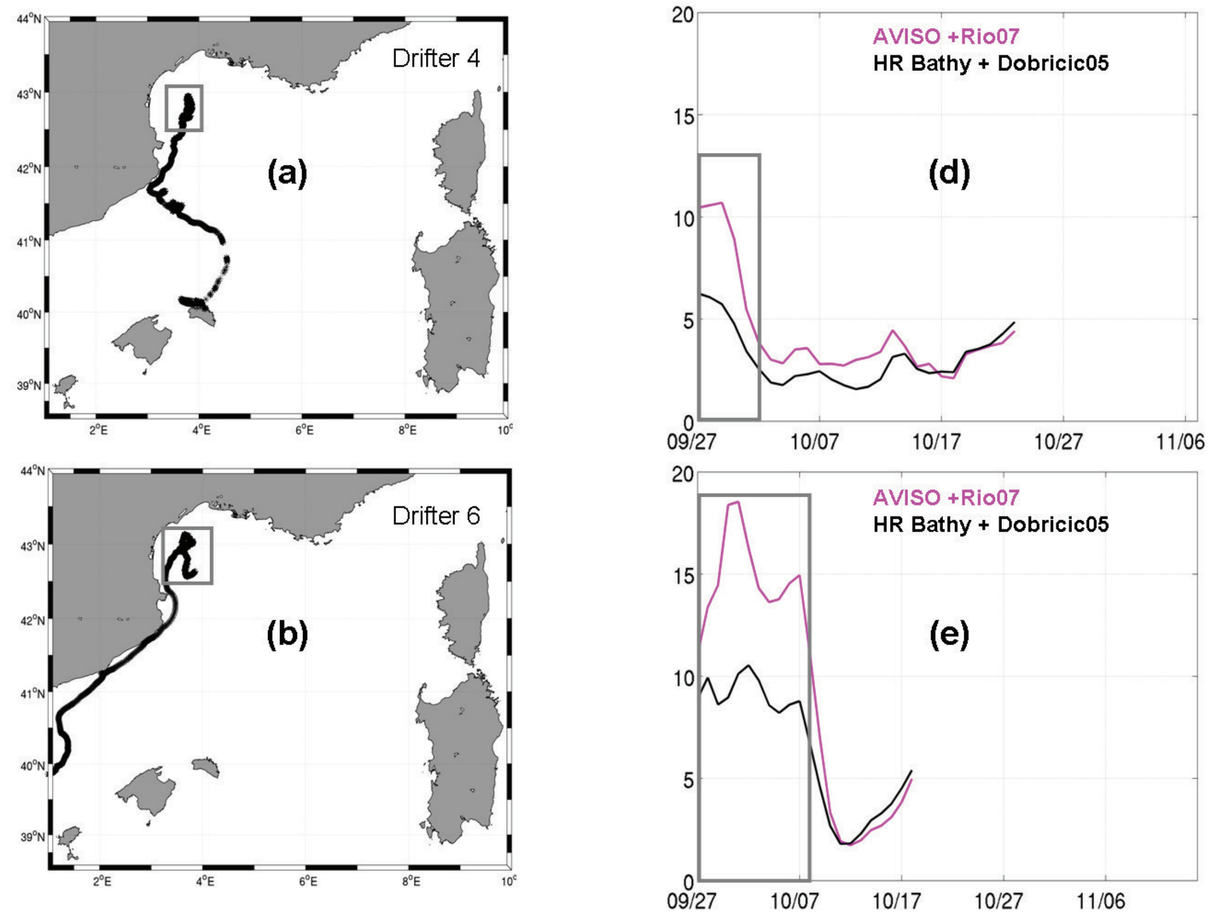

Figure 7 - Trajectories of drifters (a) 4 and (b) 6 and corresponding S_D time series (respectively (d);(e)) for the *new* - black curves - and *standard* -pink curves - altimetric products for 10 days advection-. In grey are highlighted areas (left) and corresponding periods (right) of bad S_D score

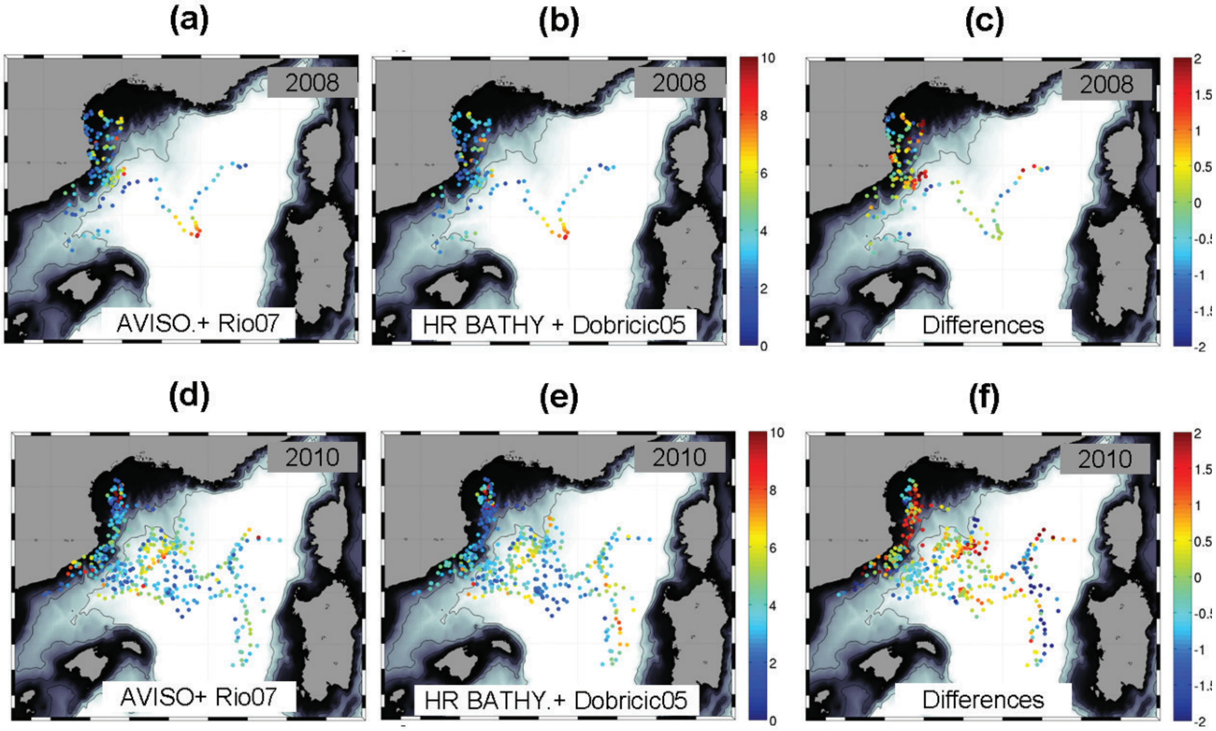

Figure 8 - Spatial distribution of S_D scores (10 days advection) along drifter daily positions for the *standard* ((a) and (b)) and *new* product ((b) and (e)) during Latex08 and Latex10. Spatial distribution of S_D differences between *standard* and *new* products for (c) Latex08 and (f) Latex10. By convention we choose each initial days of advection as drifter daily positions.

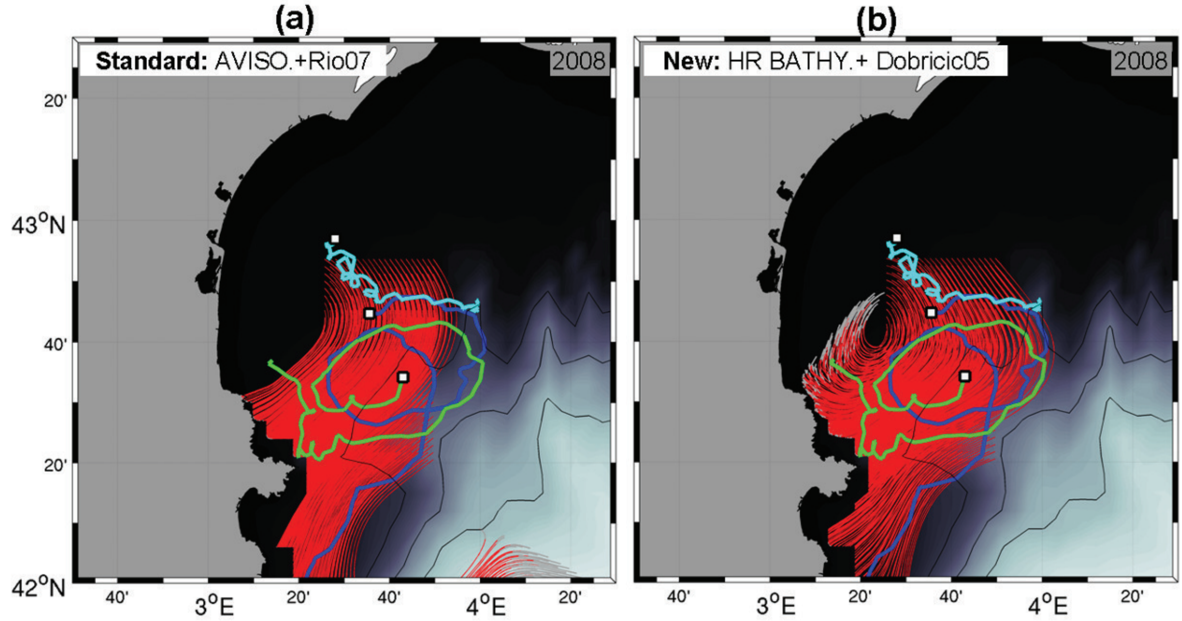

Figure 9 – Latex08 drifter trajectories (cyan, green and blue). Two drifters are trapped by the Latex eddy (in green and blue). In red are the virtual particles initially launched at drifters' trapped initial positions and 10 days advected by (a) the *standard* and (b) *new* altimetric current field. In grey are the particles trajectories for the last day of advection.

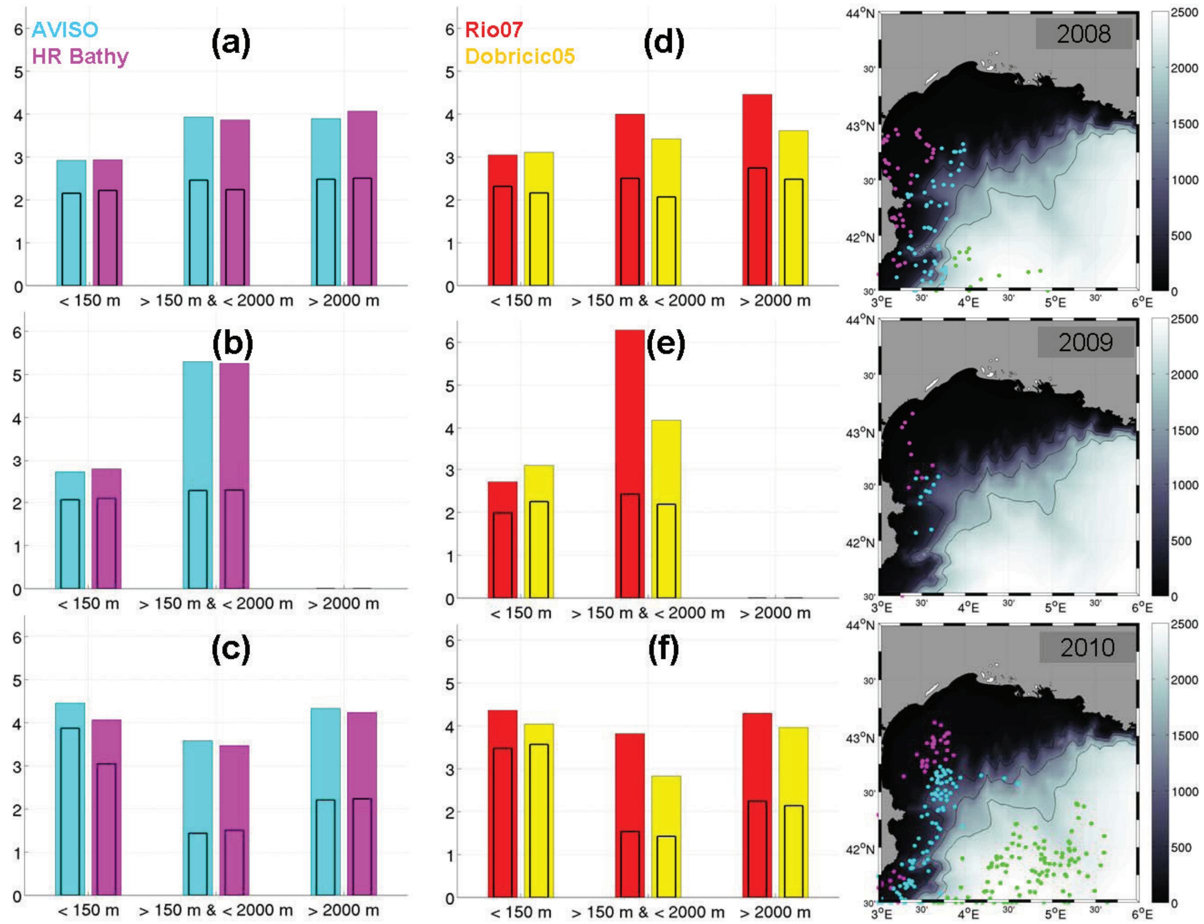

Figure 10 – (Right) Daily drifter positions used in the bathymetric classes for Latex08; Latex09 and Latex10. In pink are the points located at depths less than 150 m, in cyan the points between 150 m and 2000 m and in green the points at depths higher than 2000 m. (Left). Diagram of mean $\overline{S}$ scores with respect to Latex drifters (a, b, c) for each OI methods and (d, e, f) for each mean currents function of bathymetric classes. The large (respectively thin) diagrams correspond to $\overline{S}$ score with 10 days (respectively 3 days) advection.